Materials Science-Poland, *Vol. 27*, *No. 1*, *2009*

Investigations of highly conducting and transparent Sc doped ZnO films grown by the sol-gel process

R. SHARMA[1], P. K. SHISHODIA[2], A. WAKAHARA[3], R. M. MEHRA[1*]

[1]Department of Electronic Science, University of Delhi South Campus, New Delhi – 110 021, India

[2] Department of Physics & Electronics, Zakir Husain College,
University of Delhi, New Delhi 110 002, India

[3]Department of Electrical and Electronic Engineering,
Toyohashi University of Technology, Tempaku-cho, Toyohashi 441 8580, Japan

Highly transparent and conductive scandium doped zinc oxide (ZnO/Sc) films were prepared on Corning glass 7059 substrates by the sol-gel technique. The influence of scandium concentration (0–1.5 wt. %) and annealing temperature (300–500 °C) on the structural, optical and electrical properties was investigated. The average transmittance was found to be above 89% in the visible region. ZnO/Sc film having 0.5 wt. % of Sc and annealed at 400 °C exhibited a minimum resistivity of 3.52×10^{-4} ohm·cm. The surface morphology of these films examined by SEM and AFM revealed formation of nano rods.

Key words: *zinc oxide; scandium doping; sol-gel method; thin films*

1. Introduction

Zinc oxide (ZnO) is a technologically important material exhibiting multifunctional properties for various applications in optoelectronic devices such as solar cells [1], transparent conducting electrodes [2], heat mirrors [3] and surface acoustic wave devices [4]. Nanoscale porous structures of ZnO with a high surface area find their application in chemical sensors [5] and dye-sensitised solar cells [6]. Indium tin oxide (ITO) or tin oxide (SnO_2) materials have long been established as transparent conducting materials. Recently, ZnO has been considered as a potential alternative to ITO and SnO_2, owing to a number of advantages, namely low cost, high mechanical stability, non-toxic nature and stability under reducing hydrogen atmosphere [7, 8]. ZnO is a wide-band-gap semiconductor material with a direct band gap of 3.37 eV [9] at room temperature and an exciton binding energy of 60 meV. Its electrical and optical prop-

*Corresponding author, e-mail: rammehra2003@yahoo.com

erties can be controlled by either selecting the nonstoichiometry and/or by appropriate dopants [10]. The effect of doping with In, Al , Y, N and Ga in ZnO has been frequently reported by various research groups [11, 12] but the effect of a rare-earth impurity such as Sc has been scarcely reported [13]. The ionic radius of Sc is very close to that of Zn and this makes it compatible for doping [11]. Various techniques have been used to deposit undoped and doped ZnO films on various substrates, including spray pyrolysis [14], organometallic chemical vapour deposition [15], pulsed laser deposition [16], sputtering [17] and sol-gel process [18]. Among these, the sol-gel technique offers many advantages for the deposition of thin coatings due to its excellent control of the stoichiometry of precursor solutions, ease of compositional modifications, homogeneity, low cost, low temperature and a non-vacuum requirement [19].

This paper reports a detailed investigation of transparent and conducting scandium doped zinc oxide (ZnO/Sc) films. The films are deposited by the sol-gel technique using 2-methoxyethanol as a solvent and monoethanolamine (MEA) as a stabilizer. The effect of Sc doping on structural (preferred orientation, surface morphology), electrical (resistivity, carrier concentration and Hall mobility) and optical (transmittance, band gap) properties are reported. The variation of band gap with doping and annealing is analyzed using band gap widening and narrowing phenomena.

2. Experimental

The precursor solution was prepared from $Zn(CH_3COO)_2 \cdot 2H_2O$ (99.95%, GR, Hayashi Pure Chemical Ind. Ltd, Japan), anhydrous 2-methoxyethanol (AR, Ajax Chemicals, Australia) and monoethanolamine (MEA, CP, Bio-Lab, London). The solution containing MEA/Zn with the molar ratio of 0.2 was stirred for 5 min. An appropriate amount (0–1.5 wt. %) of $ScNO_3 \cdot 6H_2O$, purity 99.9% was introduced as a dopant. This mixture was sonicated for about 2 h. The resultant clear, transparent and homogeneous solution was used after 48 h for film deposition. Microscopic Corning glass (7059) slide substrates were cleaned ultrasonically, first in acetone and then subsequently in methanol for ten minutes each. They were further cleaned with deionised water for 20 min and finally dried in nitrogen atmosphere. The spinning speed and spin duration were 3200 rpm and 30 s, respectively. The wet films were kept to hydrolyze in air at room temperature for 5 min, then dried at 200 °C for the next 10 min and finally heated at 280 °C for 20 min in air atmosphere with the heating rate of about 10 °C/min. Thus, the drying process removes the residual organic solvents and organic groups in the deposited gel film and converts the organic precursor film into a dense inorganic film. An approximate thickness of 0.02 μm was obtained for each spin. The above process of coating and drying was repeated several times to increase the film thickness. In the present work, the thicknesses of the films were in the range of 450–500 nm. Finally the deposited films were annealed in air in the tempera-

ture range of 300–500 °C for 1 h. A slow cooling rate was maintained to avoid the possibility of stress in the films as expected in rapid cooling. Crystallite phase and orientation were evaluated by the X-ray diffraction method (XRD, Philips PW 1830 Geiger counter diffractometer, PW 1830) using a monochromatized X-ray beam with nickel-filtered CuK_α radiation (λ = 1.5418 Å). A continuous scan mode was used to collect 2θ data between 30–40°, with a 0.02 sample pitch and 4 deg/min scan rate. Microstructure was investigated by the scanning electron microscopy (SEM, JEOL JSM-6300). Average surface roughness of the films was obtained by an atomic force microscopy (AFM, Burleigh-SPI 3700) with scanned area of 5×5 μm^2. The thickness of the films was determined with a DEKTECK3-ST surface profilometer. Optical transmittance was obtained in the 300–800 nm range using a Shimadzu UV-3150 spectrophotometer. The electrical resistivity ρ and the Hall coefficient R_H were measured by the van der Pauw [20] technique. The sign of the Hall coefficient confirmed the n-type conduction of the films. The composition of scandium doped ZnO films was determined by the elemental dispersion analysis using X-ray (EDAX) measurements.

3. Results and discussion

3.1. Structural properties

Figure 1 represents the XRD patterns of ZnO/Sc (Sc – 0.5 wt. %) films as a function of annealing temperature (300 - 500 °C). It is seen from the figure that as-deposited film exhibited an amorphous nature, whereas the films annealed at 300 °C showed evidence of polycrystalline structure with (100), (002) and (101) peaks. With the increase of annealing temperature from 300–400 °C, the intensity of the (002) peak increases, indicating a c-axis preferential growth, implying an improvement in the crystalline quality of the film. With further increase in temperature > 400 °C there was a decrease in the intensity (002) peak suggesting a degradation of the films at higher annealing temperature.

Figure 2 shows the X-ray diffraction patterns of the (ZnO/Sc) films annealed at the optimized temperature of 400 °C and having different Sc concentrations. The films exhibit a dominant peak at 2θ = 34.44° corresponding to the (002) plane of ZnO and other peaks corresponding to (100) and (101), indicating the polycrystalline nature of the films. It is seen from the figure that the relative intensity of the (002)-reflection peak decreases with increasing Sc concentration greater than 1.0 wt. %. No peaks corresponding to either Sc or Sc oxides appear in the diffraction pattern of the samples, suggesting that Sc is incorporated at the Zn lattice site in the hexagonal wurtzite structure of ZnO.

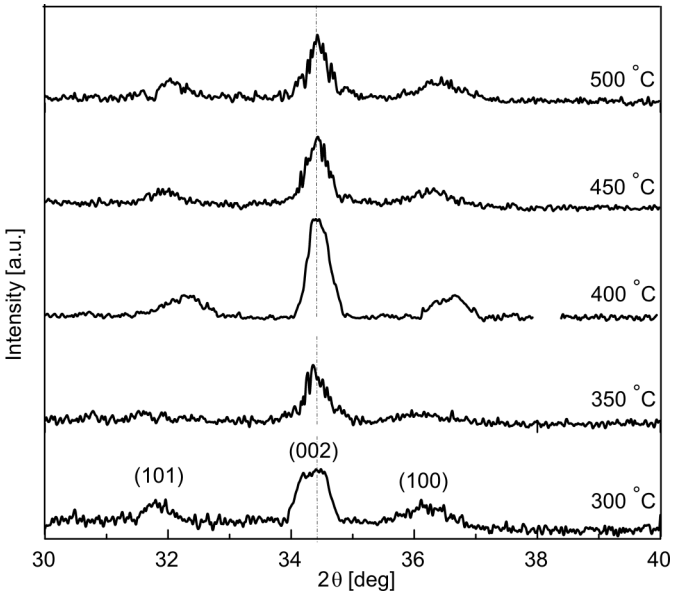

Fig. 1. Effect of annealing temperature on the XRD patterns of ZnO/Sc (Sc – 0.5 wt. %) thin films

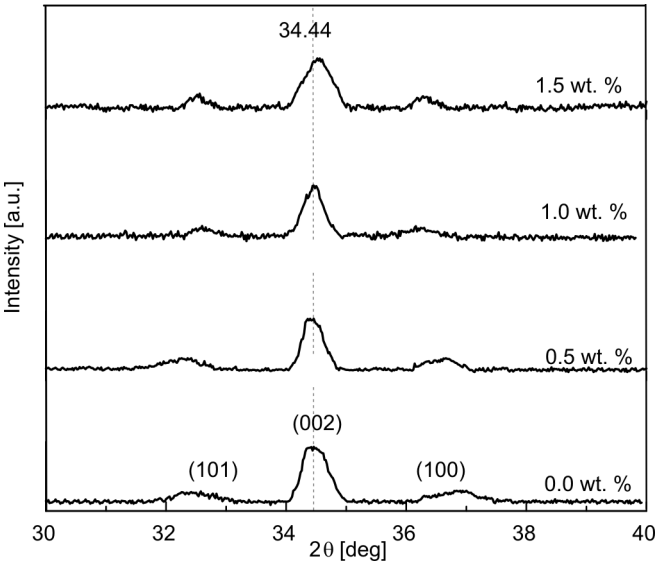

Fig. 2. Effect of doping concentration on the XRD patterns of ZnO/Sc films annealed at 400 °C in air for 1 h

Figure 3 shows the variation of grain size D and lattice constant c with annealing temperature for ZnO/Sc (0.5 wt. %) films. The grain size D of the films was calculated using the Debye–Scherrer formula [21]

$$D = \frac{0.9\lambda}{\beta\cos\theta} \tag{1}$$

where λ is the wavelength of CuK_α line, and β is the full width at half maximum (FWHM) of the (002) reflection peak.

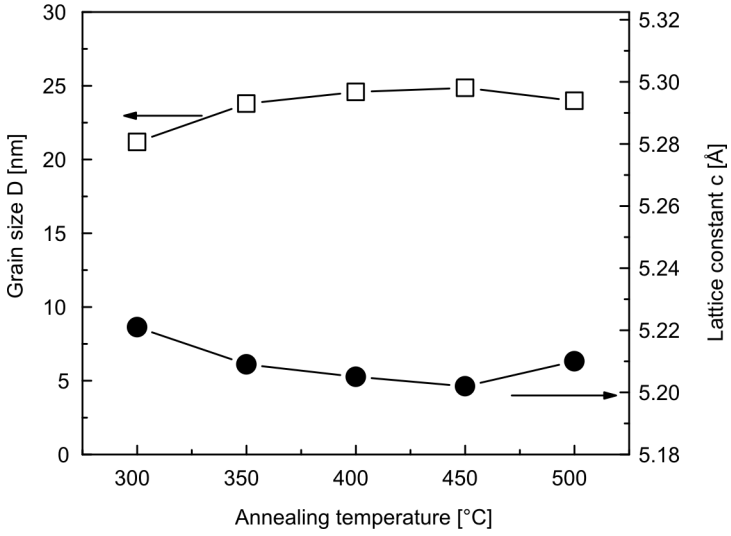

Fig. 3. Effect of annealing temperature on grain size and lattice constant of ZnO/Sc (Sc – 0.5 wt. %) thin films

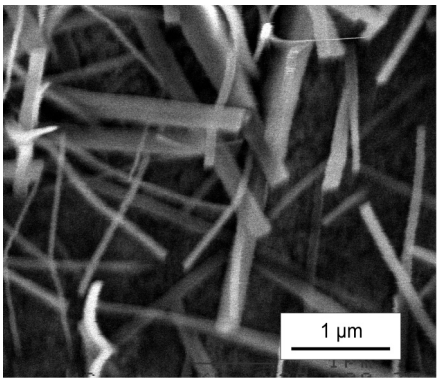

Fig. 4. SEM image of ZnO/Sc (Sc – 0.5 wt. %) thin films annealed at 400 °C in air for 1 h

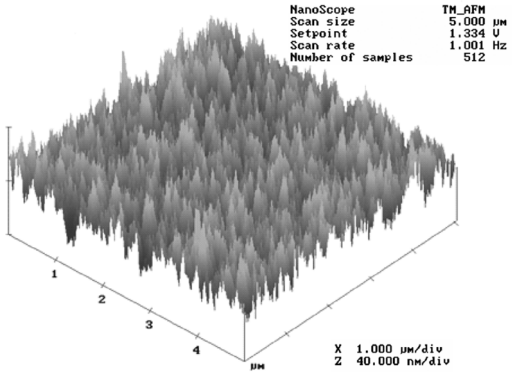

Fig. 5. AFM Image of ZnO/Sc (Sc – 0.5 wt. %) thin films annealed at 400 °C in air for 1 h

It is observed that grain size improves with the increase in annealing temperature indicating an improvement in crystallinity [22]. However, a further increase in annealing temperature above 450 °C results in a decrease in intensity and an increase in FWHM which indicate a decrease in *c* axis orientation and the grain size. It is impor-

tant to note that the value of *c* for the as deposited ZnO/Sc films is large in comparison with the unstressed bulk value of 5.2066 Å. Correspondingly, the value of *c* decreases with an increase in annealing temperature. This indicates a reduction in the tensile stress with annealing [23], which may be due to a large coefficient of linear expansion of ZnO/Sc films in comparison with the glass substrate. Thus with the increase in annealing temperature, shrinkage of *c* along with the improvement in *c* axis orientation is seen. Matsuoka et al. [24] have observed a similar shrinkage of lattice constant in Al doped ZnO films with increase of the substrate temperature.

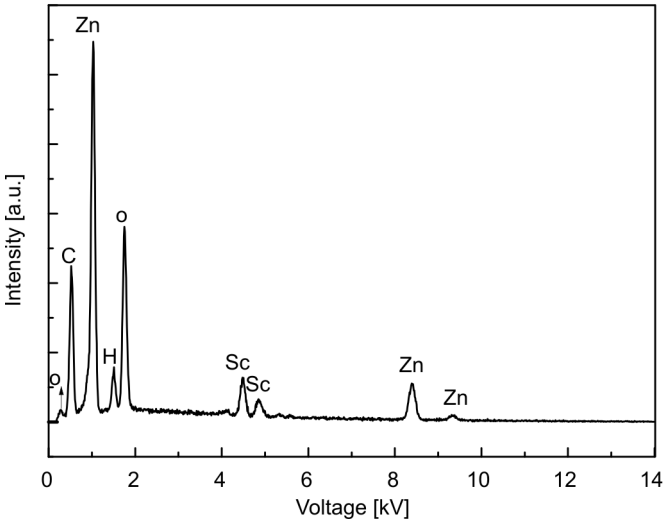

Fig. 6. Compositional analysis of ZnO/Sc (Sc – 1.5 wt. %) film annealed at 400 °C in air for 1 h

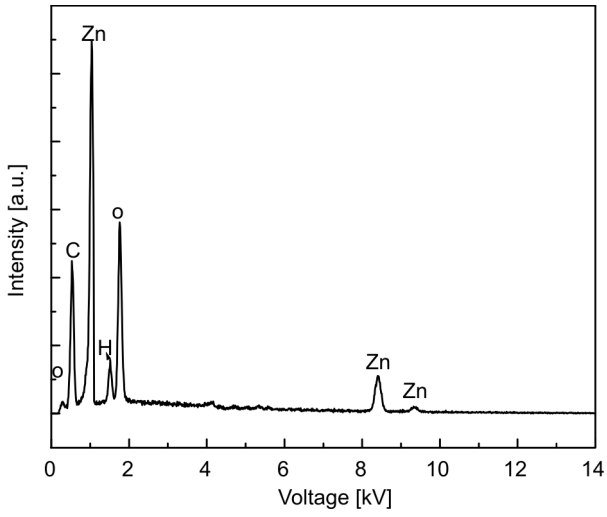

Fig. 7. Compositional analysis of ZnO film annealed at 400 °C in air for 1 h

Figures 4 and 5 show typical SEM and AFM images, respectively, of ZnO/Sc (Sc – 0.5 wt. %) annealed at the optimum temperature of 400 °C in air atmosphere for 1 h. The SEM micrograph of the film revealed the formation of nanorods. The AFM image exhibits a uniformly distributed needle type structure. The average surface roughness of the film ZnO/Sc (Sc – 0.5 wt. %) is found to be 4.81 nm.

Compositional analysis of ZnO/Sc (Sc – 1.5 wt. % and 0.0 wt. %) films, annealed at 400 °C for 1 h in air, is shown in Figs. 6 and 7, respectively. As seen from Fig. 6, the Sc doped film showed the presence of Zn, Sc and oxygen only. No other impurity was found within the EDAX detection limit. The composition (the atomic ratio of Sc to Zn) of deposited rare earth-doped ZnO films is found to be approximately equal to that in the solution. The compositional analysis of undoped (ZnO film (Fig. 7) reveals the presence of Zn and oxygen only.

3.2. Transmittance and bandgap

Transmittance spectra were recorded in the 300–800 nm range to study the influence of annealing temperature and the effect of Sc concentration on the optical properties of ZnO/Sc films. As shown in Figs. 8 and 9, all the films deposited on glass substrate exhibited high optical transparency throughout the entire visible range.

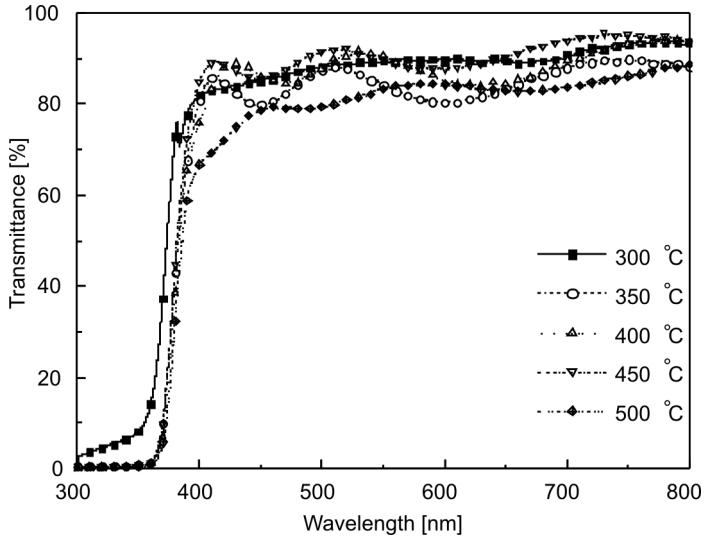

Fig. 8. Transmittance (T, %) in function of annealing temperature of ZnO/Sc (Sc – 0.5 wt. %) thin films

As shown in Fig. 8, all samples showed interference fringe patterns in the visible region of transmission spectra with an average transmittance T not lower than 89% indicating good optical quality of the deposited films with low scattering or absorption losses. The higher optical transmittance in annealed films may be due to the increased

crystal size, which reduces the inter-grain shadowing. It is observed that T increases with increase in annealing temperature up to 400 °C but with further increase in temperature it decreases. The initial increase in T is due to the improvement in the crystallinity and microstructure with an increase in annealing temperature (Fig. 8). The decrease in T with further increase in annealing temperature is due to the degradation of crystallinity of ZnO/Sc films as indicated by our XRD analysis. The transmittance is maximum for pure ZnO film and decreases with an increase in Sc concentration. The decrease in optical transmission is generally associated with the loss of light due to oxygen vacancies and scattering at grain boundaries [25]. Since all the films are deposited under similar oxygen environments and processing conditions, the loss of transmittance due to oxygen defects is assumed to be the same for all samples. The increase in scattering centres due to increased grain boundaries with an increase in Sc dopant content may be responsible for the loss of transmittance. A characteristic difference in the absorption edge has been observed with Sc incorporation in ZnO. The sharp absorption edge observed for ZnO (Sc – 0.0 wt. %) sample at 375 nm was found to shift towards blue with an increase in Sc concentration.

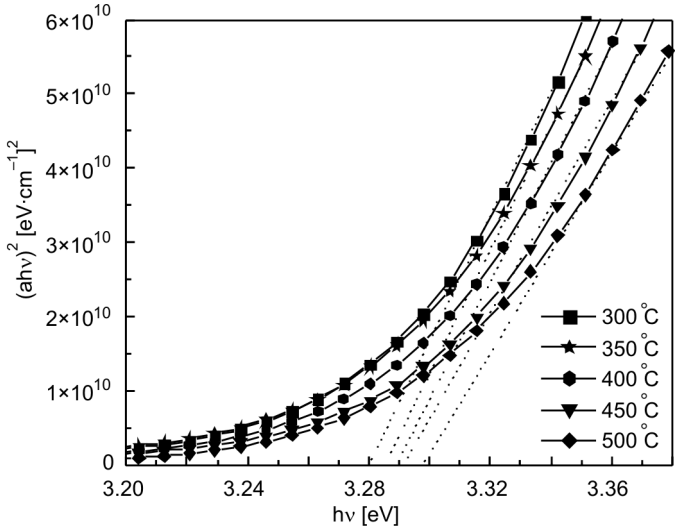

Fig. 9. Tauc's plots of ZnO/Sc (Sc – 0.5 wt. %) thin films in function of annealing temperature

The optical absorption coefficient α of a direct band gap semiconductor near the band edge, for photon energy $h\nu$ greater than the band gap energy E_g of the semiconductor, is given by [26]

$$\alpha h\nu = A\left(h\nu - E_g\right)^{1/2} \tag{2}$$

where h is Planck's constant and v is the frequency of the incident photon.

The value of α is determined from the transmittance spectra. The plot of $(\alpha h\nu)^2$ in function of photon energy $h\nu$ (Tauc's plot) for ZnO/Sc (Sc – 0.5 wt. %) films annealed at various temperatures is shown in Fig. 9 while the absorption coefficient in function of the dopant concentration for the films annealed at 400 °C is shown in Fig. 10. E_g was obtained by extrapolating the linear part of the Tauc's plot to intercept the energy axis at $((\alpha h\nu)^2 = 0$.

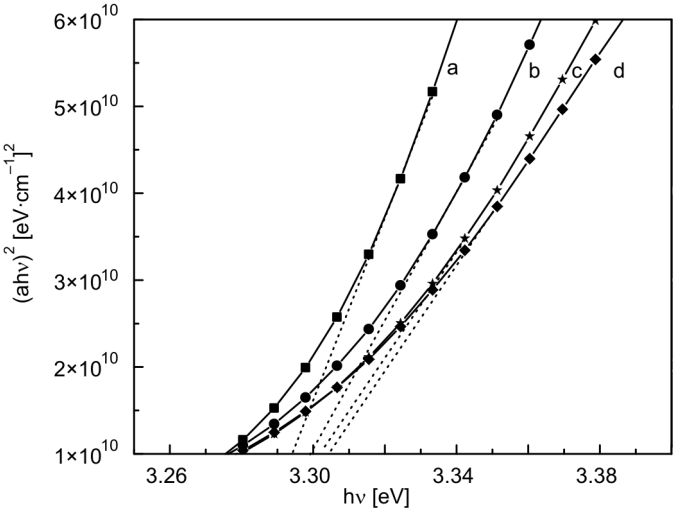

Fig. 10. Tauc's plots of ZnO/Sc films annealed at 400 °C in air:
a – 0.0 wt. %, b – 0.5 wt. %, c – 1.0 wt. % and d – 1.5 wt. %

E_g was found to increase continuously from 3.28 to 3.30 eV with an increase in annealing temperature for ZnO/Sc (Sc – 0.5 wt. %) films. The increase in E_g may be attributed to the increase in the grain size and the stress relieving process in ZnO/Sc films. An increase in E_g has also been observed with Sc doping. It increases from 3.29 to 3.31 eV as the dopant concentration is increased from 0 to 1.0 wt. %.

3.3. Electrical properties

The influence of the annealing temperature from 300 °C to 500 °C on resistivity ρ, carrier concentration n and the Hall mobility μ_H of ZnO/Sc (Sc – 0.5 wt. %) films is shown in Fig. 11. The resistivity is found to decrease with increasing annealing temperature up to 400 °C and thereafter it increases with annealing temperature. The observed decrease in resistivity can be interpreted in terms of enhanced crystallite structure of the films. A minimum resistivity of 3.52×10^{-4} ohm·cm, as well as a highest mobility value of 35.3 $cm^2/(V\cdot s)$ and carrier concentration of 3.27×10^{20} cm^{-3} annealed at 400 °C is obtained for ZnO/Sc (Sc – 0.5 wt. %).

The increased resistivity at higher annealing temperature might be due to the formation of oxygen vacancies by oxygen annihilation from the ZnO [27]. Further, the increase in resistivity of the films at temperatures above 400 °C may be due to the structural degradation as well. The mobility is found to increase with the annealing temperature up to 400 °C, which is due to the improvement of crystalline structure of the films as observed by the XRD analysis. It is also observed that *n* increases with the increase in annealing temperature.

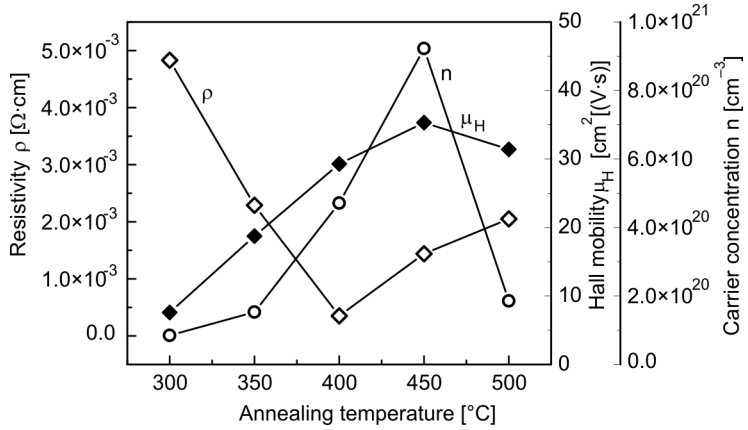

Fig. 11. Temperature dependences of σ, n and μ in ZnO/Sc (Sc – 0.5 wt. %) thin films annealed in air

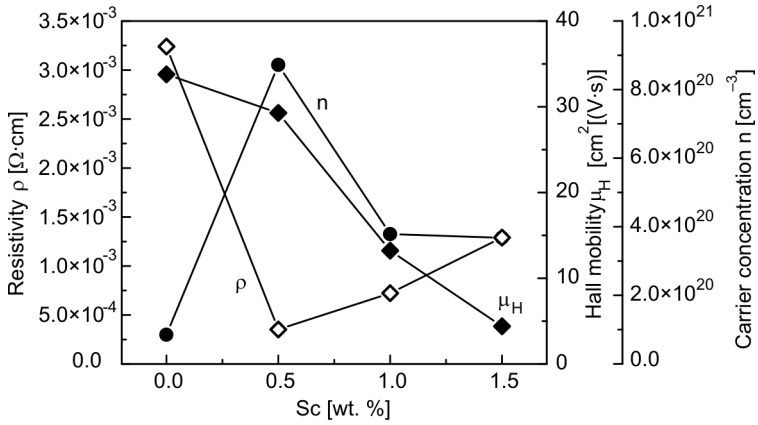

Fig. 12. Dependences of σ, n and μ of ZnO/Sc thin films annealed at 400 °C in air on Sc concentration

The variations of ρ, n and μ_H of ZnO/Sc films in function of Sc concentration are shown in Fig. 12. It is also seen from Fig. 9 that ρ decreases sharply as the Sc concentration is increased up to 0.5 wt. %, correspondingly n is found to increase while there is a gradual reduction in μ_H. The increase in n confirms that Sc acts as an effective

donor in ZnO films. The increased carrier concentration is due to the contribution from doping ion Sc^{3+}on the substitution site of Zn^{2+} ions and/or from interstitial zinc atoms. However, after 0.5 wt. % of Sc doping, the carrier concentration tends to saturate and resistivity starts increasing. This is probably because of the limited solubility of Sc in ZnO/Sc. Tang and Cameron [28] have shown a similar effect in ZnO/Al films. The impurity content dependence of mobility is not related to the crystallinity estimated by the intensity and full width at half-maximum of the (002) diffraction peak; the crystallinity did not change with increasing impurity content. The decrease in mobility at higher doping may be due to scattering from grain boundaries and defects produced by doping, which is also supported by the XRD analysis [29].

3.4. Variation of bandgap

The variation of E_g with annealing temperature and dopant concentration has been analyzed in terms of band gap widening ΔE^{BM} due to the Burstein–Moss effect and bandgap narrowing ΔE^{EX} due to many body effects. In the model of Burstein and Moss, the absorption edge shift in an n-type semiconductor is shown to be dependent on carrier concentration and is given as [30]

$$\Delta E^{BM} = \left(3\pi^2 N\right)^{2/3} \frac{\hbar^2}{2m_{vc}^*} \tag{3}$$

where m_{vc}^* is a reduced effective mass given by

$$\frac{1}{m_{vc}^*} = \frac{1}{m_c^*} + \frac{1}{m_v^*} \tag{4}$$

where m_c^* is the effective mass in the conduction band, and m_v^* is the effective mass in the valence band. The calculated value is shown in Fig. 13, which corresponds to $m_c^* = 0.38m_0$ and $m_v^* = 1.8m_0$ [31]. At higher concentrations above the Mott critical density, such as in heavily doped and highly excited semiconductors, electronic states of the crystal are modified because of carrier–carrier interaction and carrier–impurity interaction. That is, many body effects such as exchange and Coulomb interactions lead to a narrowing of the band gap [32, 33]. According to Wolf [34], in heavily n-type doped semiconductors the conduction band is shifted downwards by a quantity equal to ΔE^{EX}.

$$\Delta E^{EX} = -\frac{e}{2\pi\varepsilon_0\varepsilon_r}\left(\frac{3N}{\pi}\right)^{1/3} \tag{5}$$

where $\varepsilon_r = 8.5$ [35] is the relative electric permittivity. This band gap shrinkage represents the exchange energy due to the electron–electron interaction. The expected absorption edge shift is therefore calculated as $\Delta E = \Delta E^{BM} - \Delta E^{EX}$.

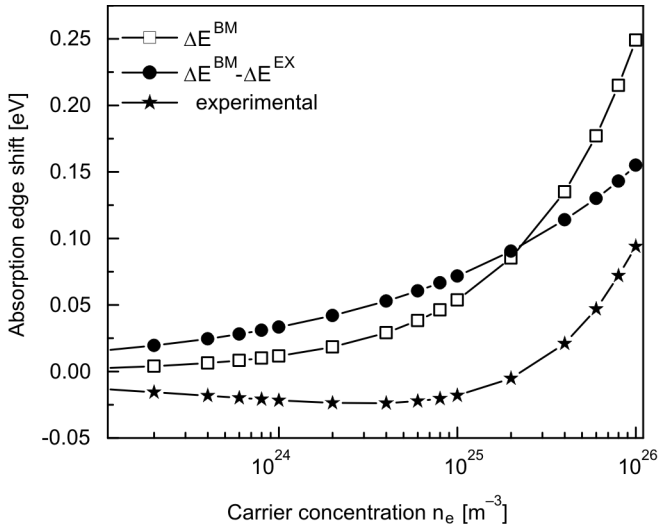

Fig. 13. Absorption edge shift ΔE in function of the carrier concentration

The theoretical and experimentalvalues of E_g in function of n are shown in Fig. 13. It is evident from the figure that the observed variation of E_g with n could not be explained by using the above mentioned two effects.

4. Conclusions

High quality *c* axis orientation Sc doped ZnO films have been deposited via the sol-gel route. The resistivity as low as 3.52×10^{-4} ohm·cm and transmittance 91% in the visible range have been achieved in these films. Such highly conducting and transparent films could be used as solar cell windows similar to ITO films.

Acknowledgement

One of the authors, Ruchika Sharma, gratefully acknowledges the financial assistance of AIEJ, Japan, during her visit to Toyohashi University of Technology, Toyohashi, Japan. The financial support of DRDO, Govt. of India, under the project No. ERIP/ER/0103325/M01 is gratefully acknowledged.

References

[1] RONOVICH J.A., GOLMOYA D., BUBE R.H., J. Appl. Phys., 51 (1980), 4260.
[2] SRIKANT V., CLARKE D.R., J. Appl. Phys., 81 (1997), 6357.
[3] MINAMI T., NATO H., TAKAT A.S., Thin Solid Films, 124 (1985), 43.
[4] CHOPRA K.L., MAJOR S., PANDYA D.K., Thin Solid Films, 102 (1983), 1.
[5] WEIBENRIEDER K.S., MULLER J., Thin Solid Films, 300 (1997), 30.
[6] SEOK-SOON K., JUN-HO Y., YUNG-EUN S., Solar Energy Mat. Solar Cells, 79 (2003), 495.
[7] MAJOR S., KUMAR S., BHATNAGAR M., CHOPRA K.L., Appl. Phys. Lett., 49 (1986), 394.

[8] HU J., GORDON R.G., J. Appl. Phys., 72 (1992), 5381.
[9] BIXIA L., ZHUXI F., YUNBO J., Appl. Phys. Lett., 79 (2001), 943.
[10] MALIK A., SECO A., NUNES P., VIEIRA M., MRS Displays Technologies, 471 (San Francisco, USA, 2–8 April 1997).
[11] TANG W., CAMERON D.C., Thin Solid Films, 238 (1994), 83.
[12] CHANG J.F., LIN W.C., HON M.H., Appl. Surf. Sci., 183 (2001), 18.
[13] MINAMI T., YAMAMOTO T., MIYATA T., Thin Solid Films, 366 (2000), 63.
[14] NUNES P., FORTUNADEO E., MARTINS R., Thin Solid Films, 383 (2001), 277.
[15] ROTH A.P., WILLIAMS D.F., J. Appl. Phys., 52 (1981), 6685.
[16] LU Y.F., NI H.Q., MAI Z.H., REN Z.M., J. Appl. Phys., 88 (2000), 498.
[17] JIANG X., WONG F.L., FUNG M.K., LEE S.T., Appl. Phys. Lett., 83 (2003), 1875.
[18] JIMÉNEZ-GONZÁLEZ A.E., SOTO URUETA J.A., SUÁREZ-PARRA R., J. Crystal Growth, 192 (1998), 430.
[19] CHATELON J.P., TERRIER C., BERNSTEIN E., BERJOAN R., ROGER J.A., Thin Solid Films, 247 (1994), 162.
[20] VANDER P., Philips Res. Repts., 13 (1958), 1.
[21] AZAROFF L.V., *Elements of X-ray Crystallography*, McGraw Hill, New York, 1968.
[22] MINAMI T., SATO H., TAKAT A.S., OGAWA N., MOURI T., Jpn. J. Appl. Phys., 31 (1992) , L 1106.
[23] TAKADA S., J. Appl. Sci., 73 (1993), 4739.
[24] MATSUOKA M., HOSHI Y., NAOE M., J. Appl. Phys., 63 (1998), 2098.
[25] SARKAR A., GHOSH S., PAL A.K., Thin Solid Films, 204 (1991), 255.
[26] SZEYRBOWSKI J., DIETRICH A., HOFFMANN H., Phys. Stat. Sol. a,78 (1983), 243.
[27] MINAMI T., YAMAMOTO T., MIYATA T., Thin Solid Films, 64 (2000), 63.
[28] TANG W., CAMERON D.C., Thin Solid Films, 238 (1994), 83.
[29] MINAMI T., NANTO H., TAKATA S., Jpn. J. Appl. Phys., 71 (1992), 880.
[30] MOSS T.S., Proc. Phy. Soc. London., B 67 (1954), 775.
[31] DIETZ R.E., HOPFIELD J.J., THOMOS G.D., J. Appl. Phys., 32 (1961), 2282.
[32] AUVERGNE D., CAMASSEL J., MATHIEU H., Phys. Rev. B, 11 (1975), 2251.
[33] MINAMI T., YAMANISHI M., KAWAMURA T., KUBO U., Jpn. J. Appl. Phys., 15 (1976), 1117.
[34] WOLF P.A., Phys. Rev., 126 (1962), 405.
[35] MAJOR S., BANERJEE A., CHOPRA K.L., Thin Solid Films, 125 (1985), 179.

Received 12 March 2008
Revised 4 September 2008